Geoacoustic inversion of ambient noise: A simple method

C. H. Harrison[1], D. G. Simons[2]

[1]SACLANT Under Sea Research Centre, Viale S. Bartolomeo 400, 19138 La Spezia, Italy. harrison@saclantc.nato.int
[2]TNO Physics and Electronics Laboratory, Oude Waalsdorperweg 63, 2509 JG The Hague, The Netherlands. simons@fel.tno.nl

Abstract

The vertical directionality of ambient noise is strongly influenced by seabed reflections. Therefore, potentially, geoacoustic parameters can be inferred by inversion of the noise. In this approach, using vertical array measurements, the reflection loss is found directly by comparing the upward with the downward going noise. Modelling and parameter searching are minimised, and the method does not require a detailed knowledge of the noise source distribution.

1. Introduction

It is well known that in shallow water the coherence and directionality of ambient noise depend on the noise source distribution and environmental parameters such as bathymetry, sound speed profile and bottom reflection properties. In general, knowing the environment, one would require a detailed model to predict noise. Nevertheless pioneering work on inverting the noise to deduce geoacoustic parameters has been successfully accomplished [1, 2, 12] in environments that are range- and azimuth-independent, and where one can rely on the sources being uniformly distributed. In [2] a vertically separated pair of hydrophones was used to measure the broad band noise coherence, which was then compared with model calculations searching over geoacoustic parameter space.

In the Mediterranean, where shipping densities are high, the uniform source distibution assumption is frequently violated. Furthermore the source distribution may change over a period of hours, and there may be more dramatic changes associated with individual ships at short ranges. For this reason an alternative method (an extension of [12]) is investigated in this paper. It is shown below that it is indeed possible to make deductions about the seabed properties *without* knowing the detailed source distribution. In fact the reflection loss versus angle can be found directly by comparing the noise intensity arriving from equal up and down elevation angles. In some applications, particularly at high frequencies, a solution in the form of a reflection loss may be more appropriate or useful than the conventional geoacoustic parameters. An additional benefit is that we do not need a detailed noise model; the penalty is that we need a vertical array to resolve angles. Here we investigate this "inversion" technique using some experimental ambient noise data from south of Sicily. Ground truth is conveniently provided by some independent conventional geoacoustic inversion experiments carried out during the same trial.

2. Theory

The array response to a directional noise field and noise coherence can be represented as a wave integral of a Green's function (Equation 9.14 of [3]) or as an integral over ray arrivals [4, 5]. Here we choose the latter approach in order to allow for spatially varying environments and source distributions as has already been developed in [6]. Generally, given a noise directionality $D(\phi, \theta)$ (a function of elevation angle θ and azimuth ϕ) and the vertical array's beam pattern $B(\theta, \theta_s)$ for each steer angle θ_s, the array response $A(\theta_s)$ is given by

$$A(\theta_s) = \int\int D(\phi,\theta)\, B(\theta,\theta_s) \cos\theta \, d\theta \, d\phi \qquad (1)$$

It is shown in [6] that the directionality $D(\phi, \theta)$ can be expressed as two terms:

$$D(\phi,\theta) = Q(\theta)\, S(\phi,\theta) \qquad (2)$$

In the equivalent formula for coherence in [5, 6] the beam pattern is simply replaced by a phase term. In equation (2), S is a complicated function of bathymetry, sound speed and noise source distribution including multiple arrivals, whereas Q is simply:

TG Leighton, GJ Heald, HD Griffiths, G Griffiths, (eds.), 'Acoustical Oceanography', Proc. Institute of Acoustics Vol. 23 Part 2, 2001.

$$\begin{aligned} Q(\theta) &= \exp(-a\, s_p), && \theta \geq 0 \\ &= R_b(\theta_b)\exp(-a(s_c - s_p)), && \theta < 0 \end{aligned} \tag{3}$$

where $R_b(\theta_b)$ is the local (within one ray cycle of the receiver) bottom (power) reflection coefficient, and θ_b is related by Snell's law to θ at the receiver. The exponential terms represent respectively the attenuations along the residual parts of the ray directly from the surface (s_p) and directly from the bottom (s_c-s_p). If we could access the directionality itself, dividing the down D by the up D would give

$$\frac{D(\phi,-\theta)}{D(\phi,+\theta)} = \frac{Q(-\theta)}{Q(+\theta)} = R_b(\theta_b)\exp(-a(s_c - 2s_p)) \tag{4}$$

Since this is true for all azimuths ϕ it is also true for the azimuth integral $\int D(\phi,\theta)\,d\phi$. Assuming that the effects of absorption over one ray cycle are small we obtain

$$\frac{\int D(\phi,-\theta)\,d\phi}{\int D(\phi,+\theta)\,d\phi} = R_b(\theta_b) \tag{5}$$

Given appropriate angular resolution in (1) we can actually measure R_b as a function of θ and hence θ_b since the beam response tends to the noise directionality D.

The reason for this simplicity, despite inclusion of spatial variation of the environment and noise source distribution, can be seen as follows. Imagine a distant point noise source from which a single ray extends, after multiple surface and bottom reflections, to the receiver. For every such ray arriving directly (i.e. most recently) from the surface, there is a corresponding ray arriving from the seabed with exactly one extra bottom reflection, the same number of surface reflections and almost the same horizontal wavenumber. Provided the environment changes only slowly over one ray cycle, the slight shifts in position of reflection points have no effect. So all distant point sources, regardless of their strength, will appear weaker by $R_b(\theta_b)$ for downward θ than for upward θ. In addition we can relax the 'distant source' condition provided the source distribution is close to uniform as in the subsequent part of [6]. Thus this approach can tolerate arbitrary arrangements of distant ships and simultaneous local or distant wind noise.

For later reference we note that the function S in (2) reduces to

$$S(\phi,\theta) = \sin\theta_t \,/[1 - R_t(\theta_t)R_b(\theta_b)\exp(-as_c)] \tag{6}$$

with R_t and θ_t being surface loss and surface angle respectively, in the case where the noise sources are uniformly distributed dipoles.

3. Experiment

In May 1999 a set of experiments (ADVENT99) was carried out near the Adventure Bank, south of Sicily. An anchored 64-element vertical array was used for the noise measurements. The same array was used in conjunction with sound sources both fixed and towed by SACLANTCEN's ship, RV Alliance, for conventional geoacoustic inversion experiments (unpublished [7]). The 62 m array was centred in the 80 m water depth, and although all 64 hydrophones were available only the middle 32 regularly spaced ones (at half metre separation) were used for these noise calculations. Noise was sampled at 6 kHz on an automatically repeated sequence of two roughly 15 second (90112 samples) windows every four minutes (at 0.5 and 3.5 min). The electronics provided a flat band between about 100 Hz and 2 kHz. Processing consisted of manually selecting portions without obvious contamination (unpublished [8]) and then beam-forming them in the frequency domain using MATLAB. The beam-formed array response can be determined conveniently by calculating the cross-spectral density between all pairs of channels, $C_{ij}(f)$, using a ready-made MATLAB routine including FFT averaging [9], then multiplying by the steer vectors $w_i(\theta_s,f)$, $w_j(\theta_s,f)$ for frequency f and summing

$$A(\theta_s, f) = \sum_i \sum_j w_i(\theta_s)\, C_{ij}(f)\, w_j(\theta_s) \tag{7}$$

An example of the beam-formed spectrum for the middle 32 hydrophones is shown in Figure 1. One can immediately see that there is more noise from above (top part of figure) than from below (bottom of figure) and that the picture is dominated by the poor angular resolution of the array at low frequencies. The design frequency of this middle part of the array is 1500 Hz and there is a clear grating lobe contribution arcing from +90° at 1500Hz to +40° at 2000 Hz. An anti-aliasing filter cuts the response off at about 2 kHz.

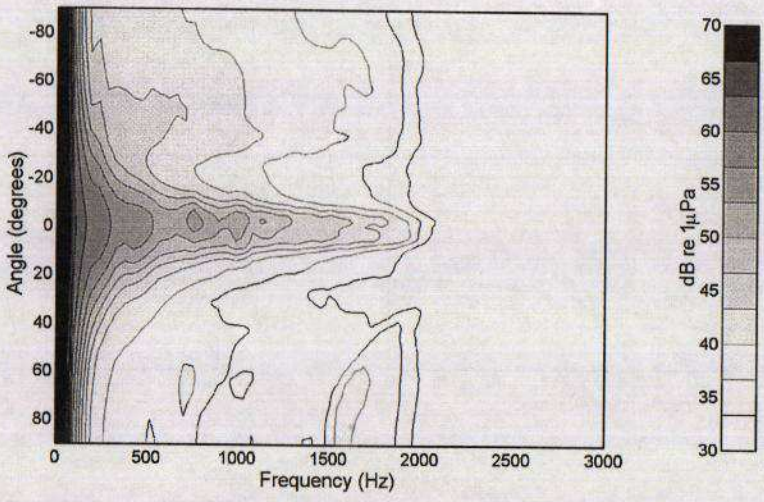

Figure 1. Beam-formed ambient noise spectrum measured on a 32-element vertical array.

The conventional geoacoustic inversion using low frequency sweeps (150-850 Hz) [7] led to the inferred optimum parameters at the ranges shown in Table 1. In the current context we regard these values as "ground truth".

Parameter	2 km	5 km	10 km
Sediment speed c_s (m/s)	1559±8	1568±7	1569±32
Sediment thickness h (m)	4.3±0.7	5.4±0.7	6.6±6.7
Attenuation α (dB/λ)	0.4±0.06	0.5±0.06	0.6±0.20
Density ρ (g/cm^3)	1.53±0.05	1.50±0.2	1.58±0.10
Sub-bottom speed c_b (m/s)	1637±17	1742±51	1702±68

Table 1. Ground truth – environmental parameter estimates taken from [7].

4. Simulation

Because of the problem of angle resolution it is wise to estimate its effect on the array response. Substituting (2) into (1) and dividing downward by upward array response we obtain the ratio of beam responses $\Re$, which is an approximation to R_b

$$\frac{A(-\theta_s)}{A(+\theta_s)} = \Re(\theta_s) \tag{8}$$

We note that, although S does not truly cancel out, its influence on the ratio $\Re(\theta_s)$ is weak. Therefore we assume that an estimate of S under the ideal conditions of a uniform noise source distribution, as in (6), will suffice. First we take the ground truth data (for 2 km) with an assumed sound speed of 1510 ms^{-1} just above the sediment, and we calculate the bottom reflection loss (RL=10log$_{10}$(R$_b$)) versus angle using SAFARI [10]. Then we substitute this into (6) with R_t=1 and $(a.s_c)\rightarrow 0$, and we calculate the array response ratio $\Re(\theta_s)$ as distinct from the directionality ratio in (5).

Figures 2(a-d) show a set of comparisons between $\Re(\theta)$ and $R_b(\theta)$ at frequencies of 100, 300, 500, 1000 Hz. One can immediately see the smoothing effect of the beam pattern. The interference nulls (caused by the interference between the upper and lower boundaries of the sediment) are covered up, and more seriously, at low frequencies the beampattern averages so much that the high loss part of the RL curve (high angles) is biased towards a low value. The only solution is to improve the angle resolution by, for instance, adaptive beam forming, or to attempt to deconvolve the known beam pattern.

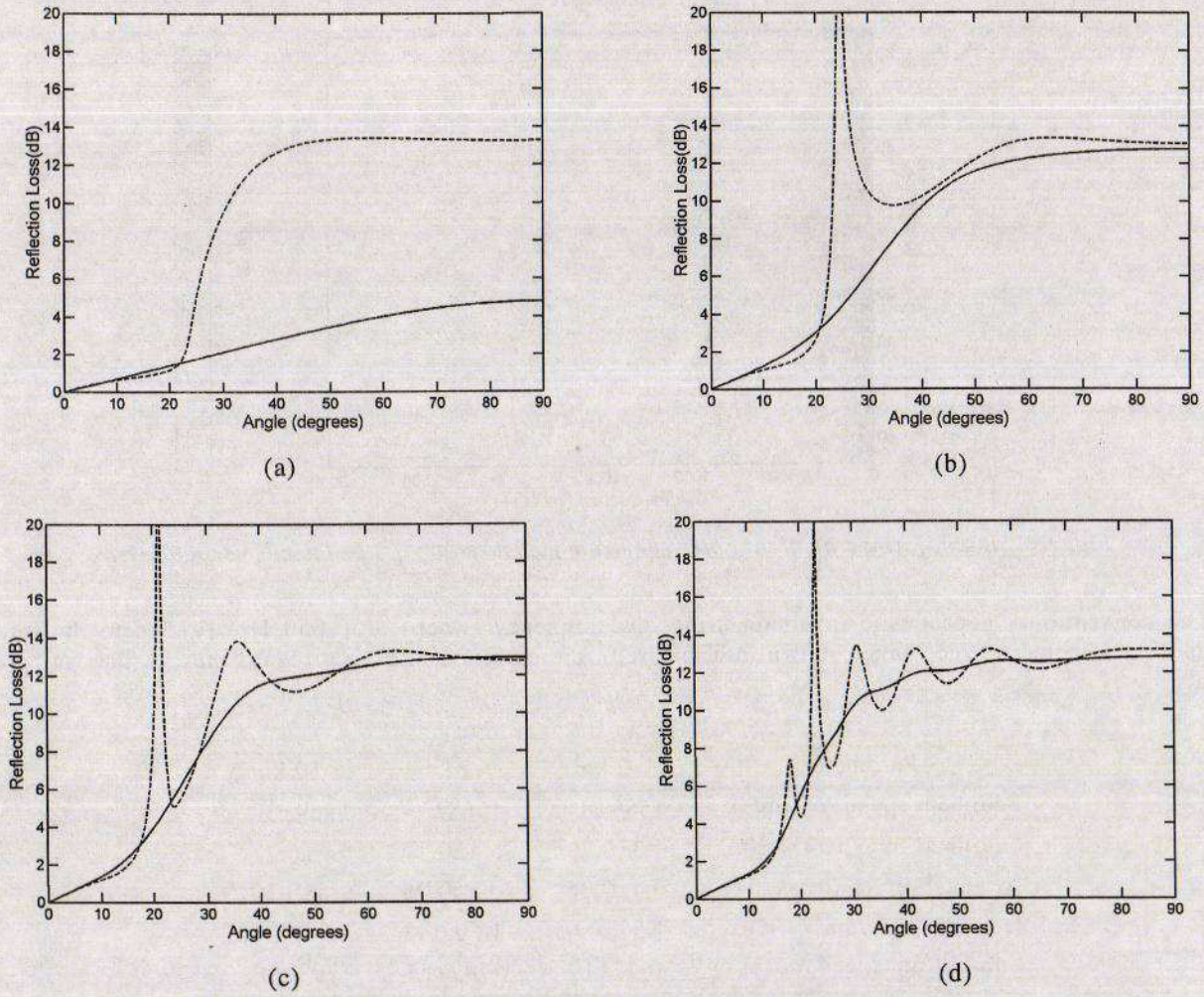

Figure 2. Reflection loss calculated with SAFARI using 'ground truth' parameters, R_b (dashed), and ratio of array responses, $\Re$ (solid); at (a) 100 Hz, (b) 300 Hz, (c) 500 Hz, (d) 1000 Hz.

The 'before' and 'after' effect on the complete reflection loss *vs* angle and frequency can be seen conveniently by first taking the formulae in Section 1.6.3 of [3] to evaluate the three layer problem, and then applying the same beam spreading to it. This is shown in Figures 3(a,b).

5. Analysis of results

We have several options with the noise data. We can collect together the usable sections of noise with the aim of averaging out local changes in directionality. Alternatively we can look at 15 second blocks of noise gathered at different times of day with the aim of checking the sensitivity of the method to changes in source distribution. In a separate experiment in the vicinity, MAPEX2000 (unpublished [11]), noise measurements made with a 256 element horizontal array detected about 14 ships passing in 4 hours. It is thought that there were no ships close enough to spoil the 'distant ship' approximation of Section 3, although clearly a non-uniform and evolving distribution is to be expected. Invariance of the quantity $\Re(\theta)$ in (8) would provide some confidence in the theory.

Figure 4(a-d) shows the quantity $10 \log_{10}\Re(\theta)$ calculated from the VLA array response according to (8) for four separate 15 second blocks each about one hour apart. (The angle has been corrected from that at the receiver to that at the seabed on the assumption that the respective sound speeds are 1505 and 1500 ms^{-1}.) The array response is calculated for 181 steer angles from the cross-spectral density (128-point FFT, sampling at 6000Hz with averaging over the 15 seconds using the MATLAB function CSD)

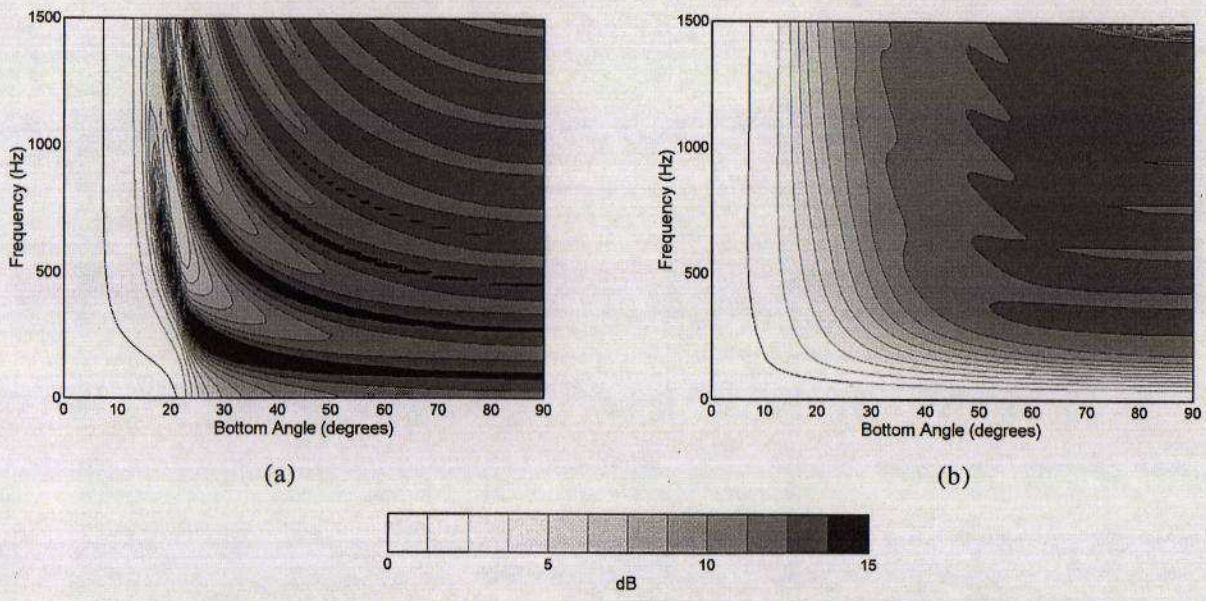

Figure 3. Reflection loss (a) calculated with 3-layer formula from [3], (b) including simulated beam forming.

Although there are slight differences the main features appear not to change with time. In contrast the array response for these same times (Figure 5(a-d)) does show significant variation particularly near horizontal. This suggests, as we hoped, that $\Re(\theta)$ does not depend on source directionality and is simply a function of the array's position.

There are some additional interesting features in Figure 4. As expected from Figure 2, at low frequencies $10 \log_{10}\Re(\theta)$ is flatter than the true $10 \log_{10} R_b(\theta)$. For frequencies between about 200 Hz and 1500 Hz (the design frequency for this vertical array) the variation with angle resembles theory. There is a slow rise in loss up to the critical angle followed by a rapid rise to a plateau beyond, as we saw in Figure 2. However the peak is not at 90°, in fact Figure 4(a), in particular, shows a hint of fringe patterns following a law of the form $f \times \sin(\theta) = \text{constant}$. Unfortunately we might expect such behaviour from modal phenomena, array side lobe phenomena or even sediment layer thickness phenomena, so we cannot use it to discriminate. Nevertheless the resemblance to the computed reflection loss versus angle and frequency shown in figure 1.24 of [3] and Figure 3 here is quite striking.

The peak value of $10 \log_{10}\Re(\theta)$ is around 10 dB, whereas the plateau in Figure 2 is at about 13dB. At these steep angles the Rayleigh reflection coefficient for a half-space simply depends on the density-sound-speed product, so there is limited scope for altering it. For instance, if we set $\rho c=2$ the bottom loss is 9.54dB. A more likely explanation for the discrepancy is the addition of non-acoustic noise to the hydrophones. This will have the effect of disproportionately boosting the weak upward-going signal, thus making the bottom appear to be a stronger reflector. It is also possible, though unlikely in these examples, that the upward-going signal is contaminated by the side lobes of the often much stronger horizontal noise.

In this experiment the data were transmitted via a radio buoy, offset horizontally from the array via a bottom cable at a nominal distance of 130 m. A potential complication is that splashes at the buoy would appear as spatially biased noise. However the direct elevation angle to the buoy is relatively small (17°). Also in Figure 5 there is no obvious single feature at a corresponding angle for all frequencies, which suggests that the buoy is not a problem.

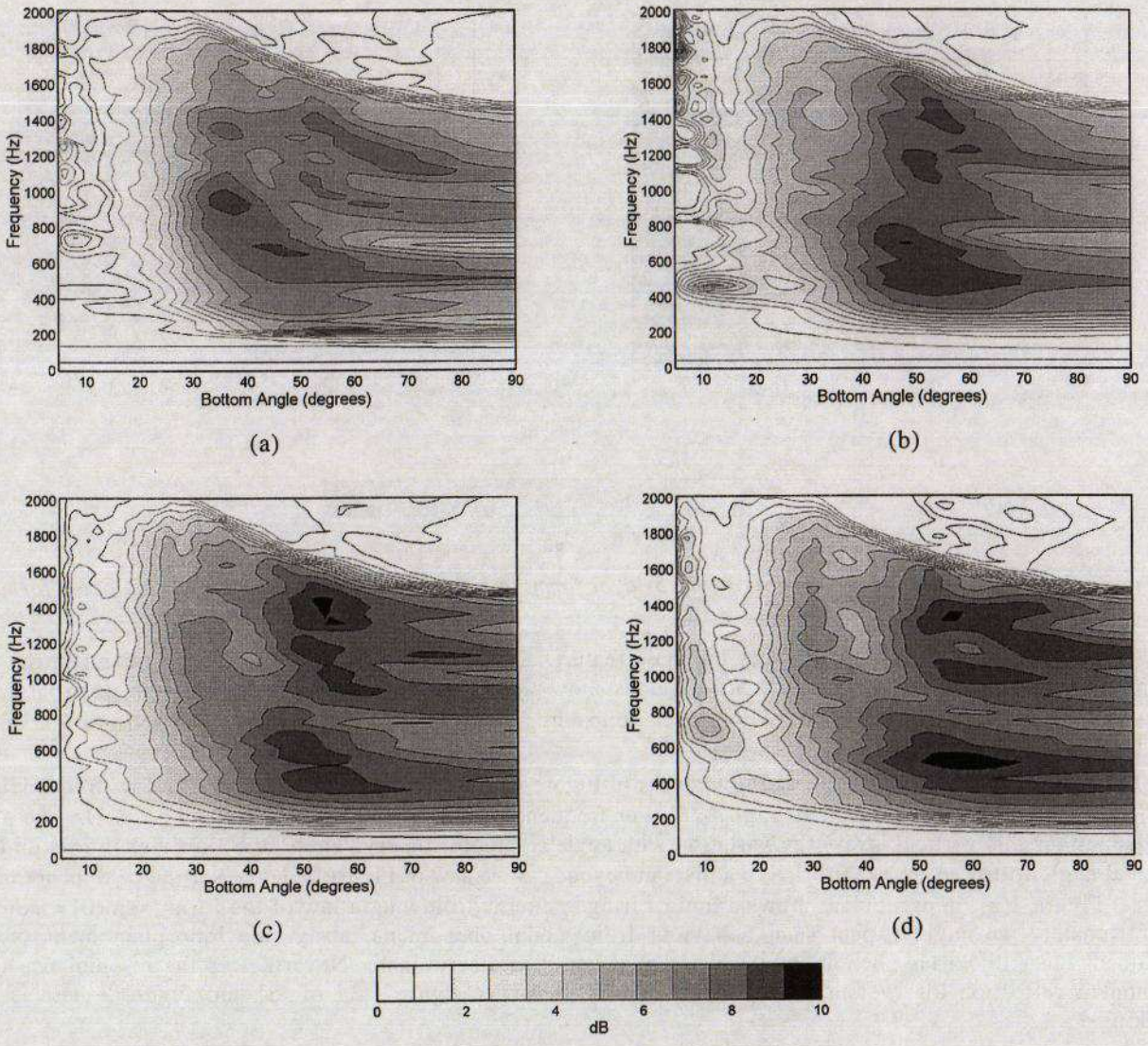

Figure 4. Inferred Reflection Loss versus angle and frequency at four times (a,b,c,d) roughly one hour apart.

Slight asymmetry of the peaks in Figure 5 will lead to an anomalous kink near zero grazing angle in reflection loss, as seen in Figure 4 (particularly (b) and (d)). A possible cause of this frequency dependent asymmetry could be that there are several distant ships contibuting from different azimuths to a slightly tilted array. Thus spectral lines from various azimuths in the horizontal plane are interpreted as deviating from horizontal in a complex manner.

Finally we form the average relection loss (Figure 6a) by first taking the power average of the four array response examples (Figure 6b).

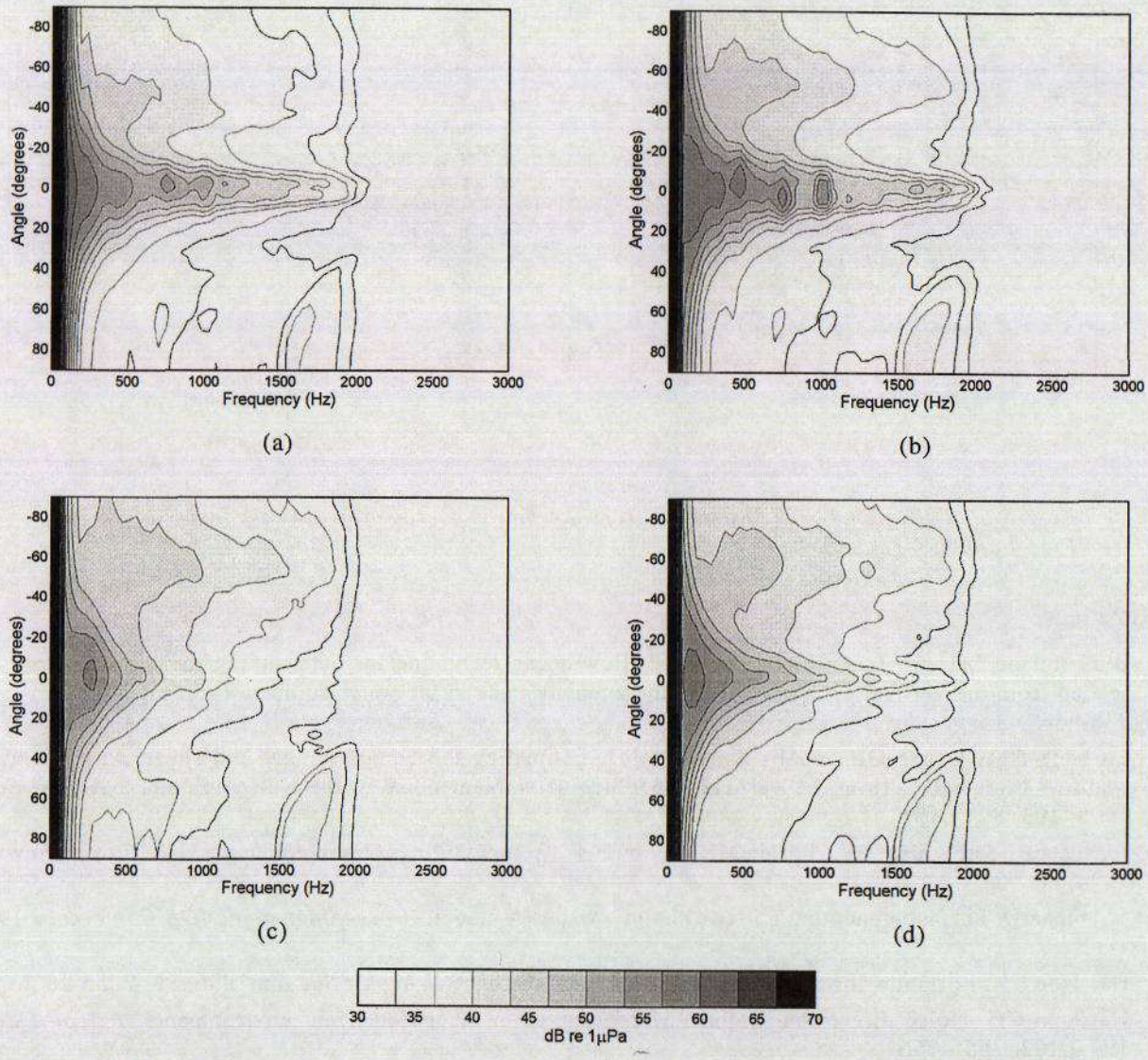

Figure 5. Beam-formed Array Response versus frequency at four times (a,b,c,d) roughly one hour apart.

6. Conclusions

A simple technique for extracting geoacoustic parameters from ambient noise measurements has been proposed and tried out with experimental data. Unlike coherence-based methods that use a hydrophone pair, this technique does not require a noise model. It can therefore still work when the noise directionality and bathymetry are unknown. The method works best at high frequencies because of the vertical array's limited angular resolution at low frequencies. Interestingly this complements conventional active inversion techniques where sound speed fluctuations impede model matching at high frequencies. It is suggested that the invariance of the inferred reflection loss (Figure 4) coupled with the variability of the array response (Figure 5) provides evidence that the method is sound. It is likely that some of the anomalies found are caused by poor quality data. For instance, the maximum value of reflection loss (at high angles) is often not as great as expected, but this can be explained by contamination with non-acoustic noise. Since first draft better quality data has been collected at several sites south of Sicily and near Elba.

Topics for further study might include detailed inversion schemes and possibly ways of counteracting the beam resolution problem.

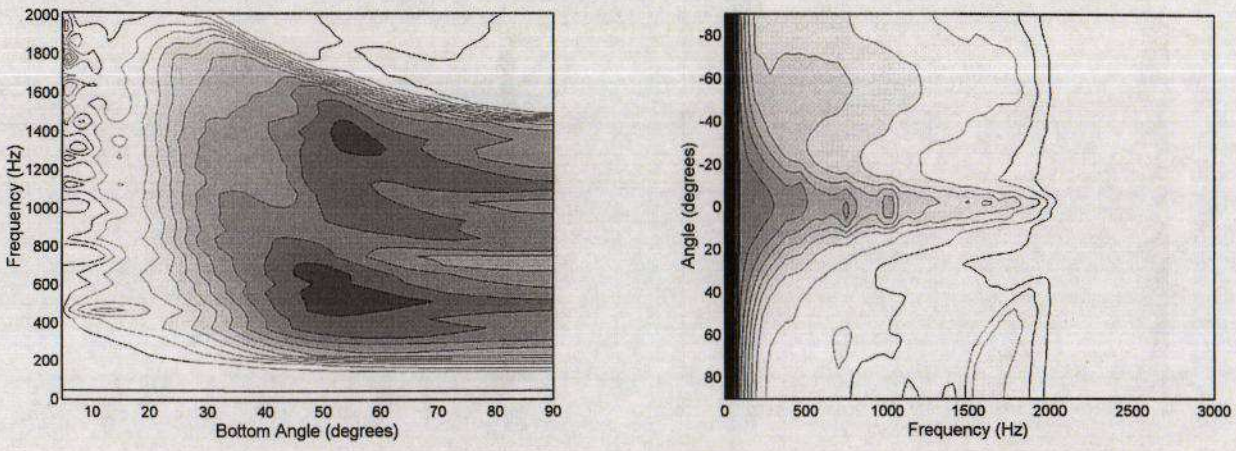

(a) (b)

Figure 6. Reflection Loss (a) derived from the power averaged array responses (b) seen in Figs 4 and 5. Grey scales unchanged.

References

[1] Buckingham MJ and Jones SAS. A new shallow-ocean technique for determining the critical angle of the seabed from the vertical directionality of the ambient noise in the water column. *J Acoust Soc Am* 1987; **81**: 938-946

[2] Carbone NM, Deane GB and Buckingham MJ. Estimating the compressional and shear wave speeds of a shallow water eabed from the vertical coherence of ambient noise in the water column. *J Acoust Soc Am* 1998; **103**: 801-813

[3] Jensen FB, Kuperman WA, Porter MB, Schmidt H. Computational Ocean Acoustics. AIP Press, New York, 1994, pp. 521

[4] Chapman D. Surface-generated noise in shallow water: A model. *Proceedings of the IOA Conference* 1988, **9**: 1-11

[5] Harrison CH. Formulas for ambient noise level and coherence. *J Acoust Soc Am* 1996; **99**: 2055-2066

[6] Harrison CH. Noise directionality for surface sources in range-dependent environments. *J Acoust Soc Am* 1997; **102**: 2655-2662

[7] Siderius Martin, Nielsen Peter, Sellschopp Jurgen, Snellen Mirjam, Simons Dick. Optimized sound propagation modeling in a time varying ocean environment. Submitted to *J Acoust Soc Am*

[8] Harrison CH. Non-acoustic interference on the 64 element VLA. SACLANTCEN Report, submitted

[9] MATLAB Signal Processing Toolbox. The Math Works Inc 1998

[10] Schmidt H. SAFARI User's Guide. SACLANTCEN Report SR-113, 1988.

[11] Harrison CH. Noise measurements during MAPEX2000, SACLANTCEN Report, submitted

[12] Aredov AA, Furduev AV. Angular and frequency dependencies of the bottom reflection coefficient from the anisotropic characteristics of a noise field. *Acoustical Physics* 1994; **40**: 176-180.